ELSEVIER

Thermochimica Acta 267 (1995) 239–248

thermochimica acta

Dynamic analysis of the melting behavior of polymers showing polymorphism observed by simultaneous DSC/X-ray diffraction measurements[1]

Hirohisa Yoshida

Department of Industrial Chemistry, Tokyo Metropolitan University, Minami-Osawa, Hachiouji, Tokyo 192-03, Japan

Received 1 November 1994; accepted 23 January 1995

Abstract

The melting behavior of isotactic poly(propylene) (iPP) and poly(vinylidene fluoride) (PVDF), which contained several crystal modifications, was measured by simultaneous differential scanning calorimeter (DSC)/wide angle X-ray diffraction (WAXD) measurements. The DSC heating curve of iPP showed at least two endothermic peaks and one exothermic peak. These peaks were assigned to melting of β- and α-modifications of iPP and melt-recrystallization of α-modification which occurred immediately after starting the melting of β-modification. The DSC heating curve of a polymer blend of PVDF/poly(methylmethacrylate) (PMMA) (PVDF content was 80 wt%) showed three endothermic peaks, which were assigned to melting of I(β), II(α) and III(γ)-modifications of PVDF, respectively. The prepared PVDF/PMMA blend film originally contained these three modifications.

Keywords: DSC/X-ray diffraction; Melting; Polymer

1. Introduction

As the crystalline phase of polymeric materials is a quasistable state, the melting process is generally observed over a wide temperature range. Furthermore, it is usually difficult to understand the structural changes during melting, since a reorganization of molecules such as cold-crystallization and melt-recrystallization occurs during the melting process of polymeric materials. In addition to the complexity of melting behavior, the melting behavior of polymeric materials is easily affected by the thermal history.

[1] Presented at the 30th Anniversary Conference of the Japan Society of Calorimetry and Thermal Analysis, Osaka, Japan, 31 October–2 November 1994.

SSDI 0040-6031 (95) 02482-4

Differential scanning calorimeter (DSC) is one of the most convenient instruments to determine phase transition phenomena and is used in various scientific and industrial fields. However, completely different results are often observed when DSC measurements are carried out at different scanning rates, because DSC measurement is a dynamic measurement. In addition, the polymers containing crystal polymorphism demonstrate transformation among different crystal modifications and melt-recrystallization during melting. Such phenomena make it difficult to analyze the melting DSC curve of polymeric materials, since the DSC curve shows several endothermic and exothermic peaks.

The combined use of DSC measurement and X-ray scattering measurement was originally employed to analyze such complex melting behavior of polymeric materials. In such cases, however, it is important to consider whether both results are comparable or not in the time scale of the measurement and thermal history of the sample. In order to avoid these problems, several attempts at simultaneous DSC/X-ray scattering measurement have been reported for polymeric materials [1–3] and lipids [4,5] utilizing synchrotron radiation. We have reported the conformational transition of gellan gum observed by the combined use of the high sensitive DSC and the simultaneous DTA/small angle X-ray scattering method [6]. Recently, we have reported the exclusive simultaneous DSC/X-ray measurement system which shows comparable accuracy and reproducibility with conventional DSC [7]. In this study, the melting behaviors of isotactic polypropylene and poly(vinylidene fluoride) are analyzed by a simultaneous DSC/wide angle X-ray diffraction (WAXD) measurement system.

2. Experimental

2.1. Sample

Isotactic polypropylene (iPP, Chisso Co., Ltd., $M_v = 2.0 \times 10^5$, isotacticity; 95%) was crystallized under the following conditions. This material (0.23 mm thickness sheet) was melted at 473 K in a hot press, and crystallized under temperature gradient conditions where the temperature of the upper press and the lower press was controlled at 438 K and 338 K, respectively. Preliminary wide angle X-ray analysis suggested that the iPP (TG-iPP) film obtained (mostly the β-modification *trans* crystal in which the a-axis was aligned along the film thickness and the c-axis was aligned parallel to the film surface) contained a small amount of α-modification. The other sample was prepared by quenching from the melt (Q-iPP). Preliminary X-ray and polarized microscopic observation suggested that Q-iPP contained spherulite which was formed only by β-modification.

Poly(vinylidene fluoride) (PVDF, Kureha Chemical Industry Co. Ltd., $M_n = 2.6 \times 10^5$) and poly(methylmethacrylate) (PMMA, bulk polymerized and fractionated, $M_n = 1.5 \times 10^5$, $M_w/M_n = 1.5$) blend film was obtained by the solvent casting method from 5 wt% *N,N'*-dimethylacetamide solution at 333 K. The PVDF content of blend film was 80%. The PVDF/PMMA blend film obtained was annealed at 428 K for 6 h before the simultaneous DSC/WAXD measurement.

2.2. Instrument

The simultaneous DSC/WAXD measurement system, which was controlled by a Seiko thermal analysis system SSC5200H, was installed on the goniometer of a Mac Science X-ray measurement system SRAMXPl 8 (a self-rotating anode type X-ray generator). The detail of the DSC/WAXD system was reported previously [7]. A film sample, 6 mm diameter, which was held between two sheets of 10 μm thick aluminum film, was clamped in a modified DSC sample vessel which had a hole of 3.0 mm of diameter at the center.

DSC scanning was carried out at 1 K min^{-1} and 0.5 K min^{-1} under a flowing nitrogen gas atmosphere. The DSC signal was stored at 0.1 s intervals. WAXD profiles were measured using a scintillation counter in conjunction with a pulse height analyzer at 0.004° of sampling time. The monochromated and pinhole collimated CuKα line generated at 40 kV and 400 mA, the wavelength of the X-rays was 0.15405 nm. A radial diffractometer scanned in the 2θ range from 13° to 23° and from 8° to 28° at 10° min^{-1} for iPP and PVDF/PMMA blend, respectively. Under these scanning conditions, one WAXD data corrected at 1.1 K and 2.1 K intervals for iPP and PVDF/PMMA, respectively.

3. Results and discussion

3.1. Isotactic poly(propylene)

It is known that iPP forms three different crystal modifications such as monoclinic α-, hexagonal β- and trigonal γ-modifications depending on the crystallization conditions and isotacticity [8,9]. The α-modification is obtained by slow cooling from the melt, and the β-modification is obtained by isothermal crystallization under 405 K and crystallization under temperature gradient conditions from the melt [10,11]. The melting behavior

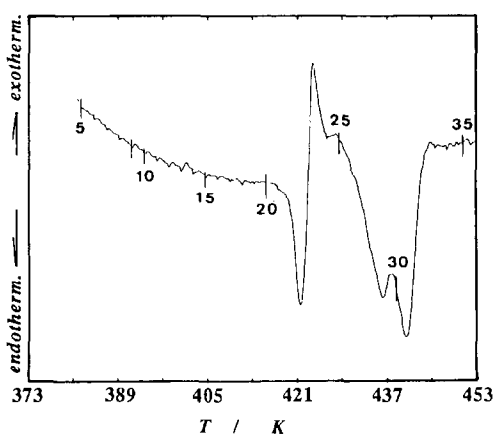

Fig. 1. DSC heating curve of TG-iPP observed by simultaneous DSC/WAXD at 1 K min^{-1}.

of the β-modification is reported by several researchers [12–14]. When the β-modification iPP is heated at a slow rate, melting and the crystallization, which is the transformation from β-modification to α-modification, occur at the same temperature.

The DSC heating curve of TG-iPP observed by the simultaneous DSC/WAXD measurement was shown in Fig. 1. The spike noise observed on the DSC base line was caused by closing the shutter of the X-ray beam. When the sample was irradiated by the X-ray beam, the DSC base line shifted to the exothermic side due to absorption of the X-ray beam. The DSC heating curve shows four endothermic peaks observed at 421, 426, 436

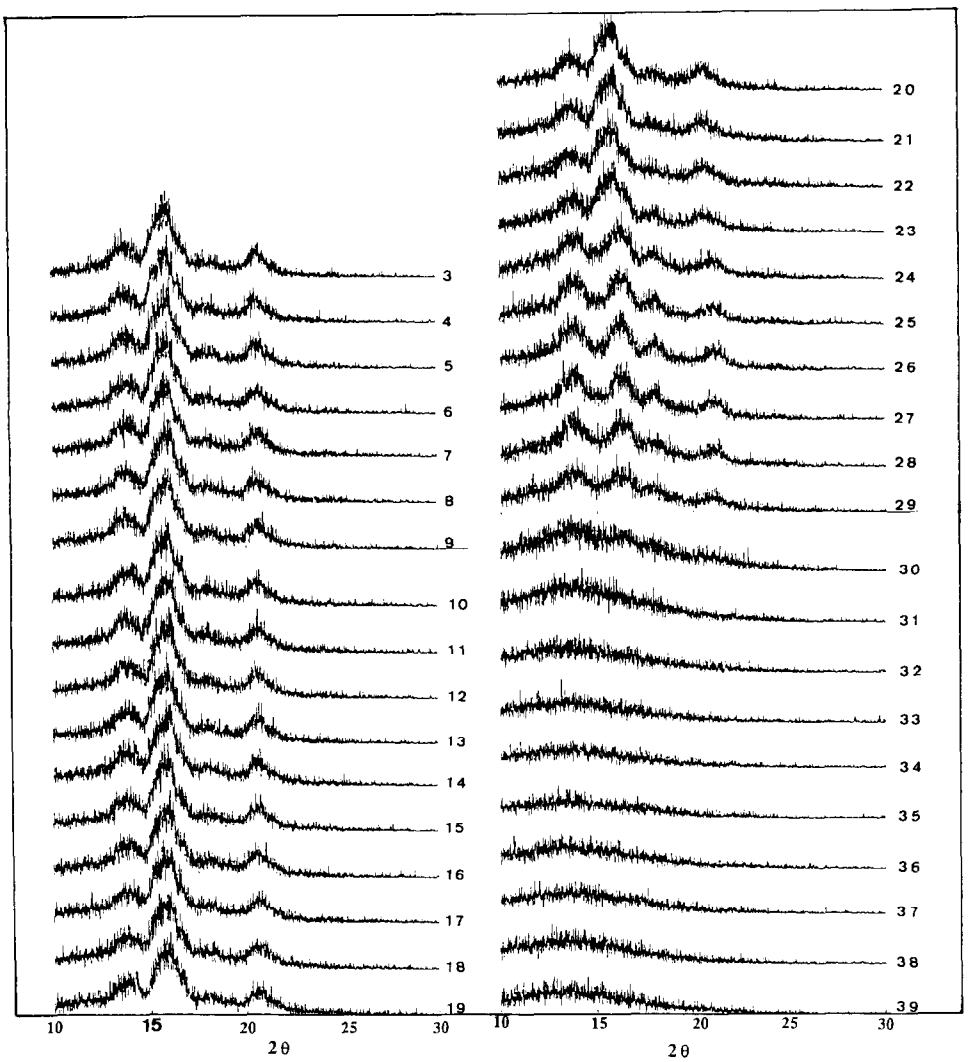

Fig. 2. WAXD profiles of TG-iPP observed by simultaneous DSC/WAXD at 1 K min^{-1}. Numbers in the figure correspond to those on the DSC curve shown in Fig. 1.

and 440 K, and one exothermic peak at 424 K. This DSC result was agreed with the result of TG-iPP observed at a heating rate of 1.25 K /min^{-1} reported by Yamamoto et al. [14]. According to Yamamoto et al. [14], two endothermic peaks observed at 421 K and 426 K are due to melting of the β-modification which is essentially one endothermic peak but is divided by the exothermic peak due to melt-recrystallization of the α-modification. Another two endothermic peaks observed at 436 K and 440 K are the melting of the originally presented α-modification and re-crystallized α-modification, respectively.

WAXD profiles of TG-iPP observed by simultaneous DSC/WAXD measurements is shown in Fig. 2. The numbers shown in Fig. 2 correspond to those on the DSC heating curve shown in Fig. 1. The WAXD profiles 3–19 in Fig. 2 suggest that TG-iPP contained both α-modification and β-modification because the diffraction peak at 15.9° was assigned to the (3 0 0) plane of the β-modification and the diffraction peaks at 14 and 16.7° were assigned to the (1 1 0) and (0 4 0) planes of the α-modification, respectively. The diffraction peak corresponding to the β-modification almost disappeared at 423 K, which was close to the exothermic peak temperature (note the WAXD profiles 23 and 24). As can be seen in the WAXD profile 24, however, the diffraction peak at 15.9° remained as a shoulder of the diffraction peak at 16.7° at 426 K. The diffraction peaks assigned to β-modification completely disappeared in the WAXD profile 25. These results indicate that two endothermic peaks and one exothermic peak observed in the temperature range from 415–429 K were essentially composed of the endothermic peak due to melting of the β-modification and the exothermic peak due to the recrystallization of the α-modification.

For the WAXD profiles 26–28 in Fig. 2, the diffraction peak at 14° became sharp with increasing temperature. This result suggests that the endothermic peaks at 436 and 460 K were due to the melting of small and large α-modification crystals, respectively. Further quantitative analysis required a high intensity and accuracy of WAXD measurement. The WAXD profiles 30 and 31 suggested the melting of the α-modification finished at 440 K which was the peak temperature of the final endothermic peak. The DSC heating curve of Q-iPP observed by DSC/WAXD at 0.5 K min^{-1} is shown in Fig. 3. Two endothermic

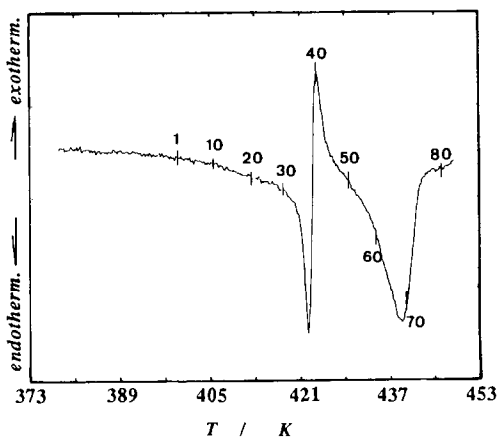

Fig. 3. DSC heating curve of Q-iPP observed by the simultaneous DSC/WAXD at 0.5 K min^{-1}.

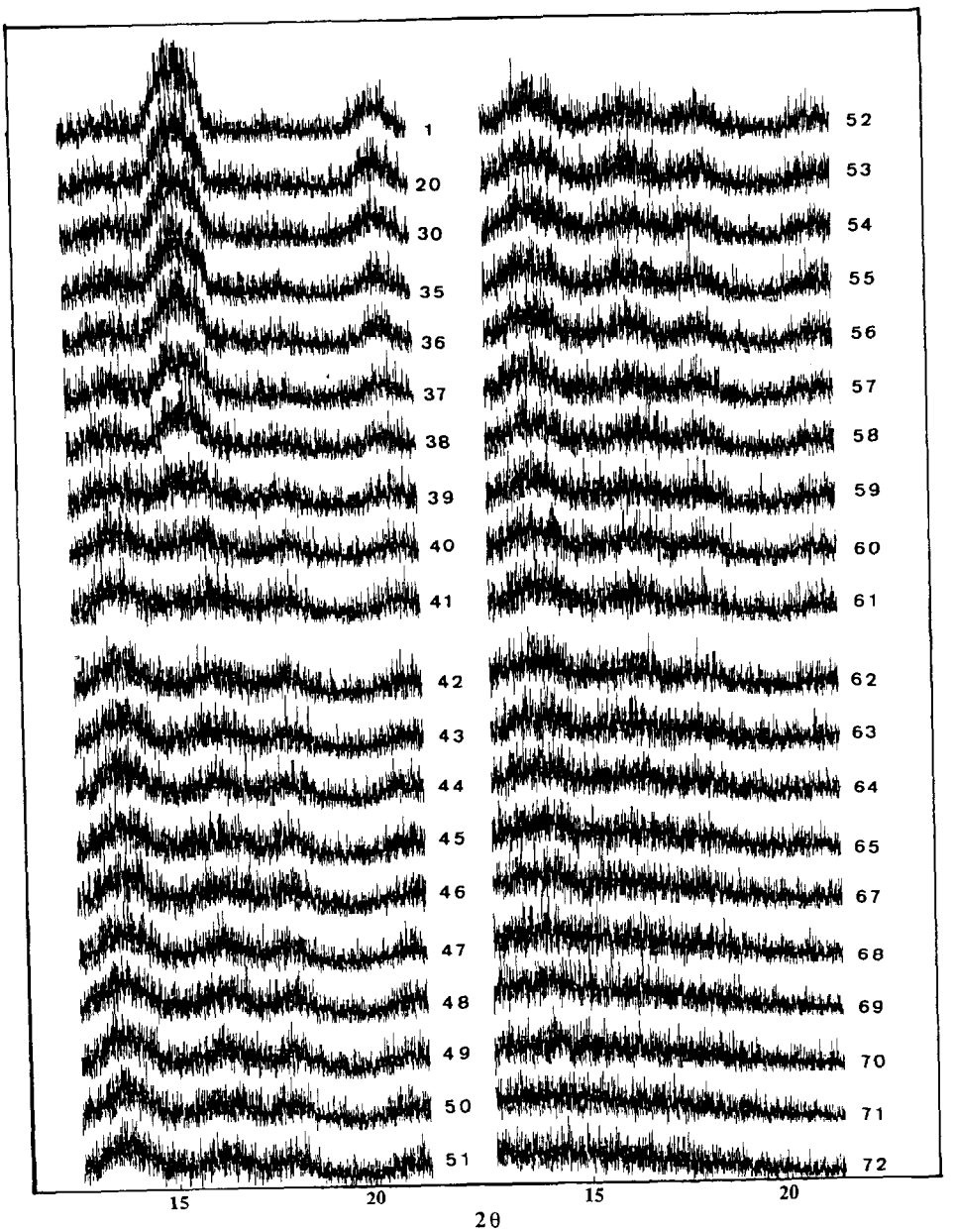

Fig. 4. WAXD profiles of Q-iPP observed by simultaneous DSC/WAXD at 0.5 K min^{-1}. Numbers in the figure correspond to those on the DSC curve shown in Fig. 3.

peaks at 422.7 K and 439.6 K and one exothermic peak at 424 K were assigned to the melting of the β-modification and the α-modification and the recrystallization of the α-modification, respectively. The heat of recrystallization of the α-modification calculated from the exothermic peak (9 J g^{-1}) showed large disagreement with the heat of melting of the α-modification (40 J g^{-1}). The corresponding WAXD profiles are shown in Fig. 4. Under these measurement conditions, one WAXD profile was obtained at a 0.6 K interval. The WAXD profile 1 suggested that Q-iPP contained only the β-modification. However, the diffraction peak at 14° appeared in the WAXD profile 20, at a temperature slightly higher than the starting temperature of melting of the β-modification. This result suggests that the recrystallization of the α-modification occurred immediately after the start of melting of the β-modification. This result also explains the disagreement of transition heat between recrystallization and melting of the α-modification. That is, the recrystallization of the α-modification proceeded at the same time as the melting of the β-modification. The exothermic transition already overlapped with the endothermic transition at 412 K. As suggested by WAXD profiles 30–42, the diffraction peak at 15.9° assigned to the β-modification decreased and the diffraction peaks at 14 and 16.7° increased with increasing temperature. The diffraction peak of the β-modification disappeared completely at 425 K (WAXD profiles 41 and 42).

The DSC heating curves of Q-iPP observed by DSC/WAXD at 0.5 K min^{-1} (a) and 1 K min^{-1} (b) are shown in Fig. 5. The starting temperature and the peak temperature of each endothermic peak observed at different heating rates showed good agreement with each other. By reflecting the dynamic process of crystallization, however, the peak temperature of the exothermic peak observed at 0.5 K min^{-1} was 0.5 K lower than that of the exothermic peak observed at 1 K min^{-1}.

3.2. PVDF/PMMA blend

It is well known that PVDF forms at least five different crystals depending on molecu-

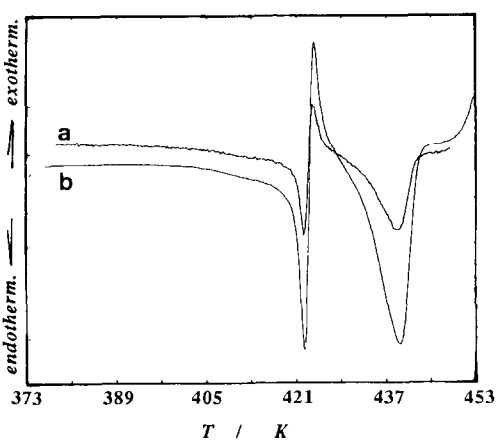

Fig. 5. DSC heating curves of Q-iPP observed by simultaneous DSC/WAXD at 0.5 K min^{-1} (a) and 1 K min^{-1} (b).

lar conformation and packing in the crystal. In particular, monoclinic II(α) in which molecules with TGTG′ conformation are packed anti-parallel to each other, orthorhombic I(β) in which molecules with all-*trans* conformation are packed parallel to each other, and monoclinic III(γ) in which molecules with T_3GT_3G' conformation are packed parallel to each other are obtained under the usual conditions [15,16]. The most stable crystal II(α) modification is obtained by cooling from the melt. Various melting temperatures of II(α), I(β) and III(γ) have been reported by several researchers, since those melting temperatures are easily affected by thermal history. PVDF conformation is influenced by mixing PMMA, because of the interaction between hydrogen atoms of PVDF and carbonyl groups of PMMA [17]. At a certain range of PMMA concentration in PVDF/PMMA blend, I(β) modification is obtained selectively by cooling from the melt. The DSC heating curve of several PVDF/PMMA blend samples shows multiple endothermic peaks which depend on the thermal history of the sample [18].

The DSC heating curve of PVDF/PMMA blend (80 wt% of PVDF) annealed at 428 K for 8 h observed by the DSC/WAXD at 1 K min^{-1} is shown in Fig. 6. Three endothermic peaks were observed at 430, 446.3 and 456.3 K. With increasing annealing time at 428 K, the endothermic peak at around 430 K became large, however, the endothermic peaks at 446 K and 456 K scarcely changed.

WAXD profiles of PVDF/PMMA blend observed by DSC/WAXD are shown in Fig. 7. The numbers in Fig. 7 correspond to those indicated on the DSC heating curve shown in Fig. 6. Although WAXD profiles were not clear because of low crystallinity of PVDF, the WAXD profiles 4–15 showed a broad diffraction peak at around 17° and a small diffraction peak at 20°. With increasing temperature the diffraction peak at around 20° shifted to the lower scattering angle side and the peak intensity decreased in the temperature range from 415 to 435 K (WAXD profiles 17–25). According to Lovinger [19], the diffraction peaks of (1 1 0) and (2 0 0) of I(β)-modification overlap at 20.6°, and the diffraction peaks of (1 0 0), (0 2 0) and (1 1 0) of the II(α)-modification appear at 17.3, 18.5 and 19.4°, respectively. As can be seen in WAXD profiles 16 and 17, the diffraction peak

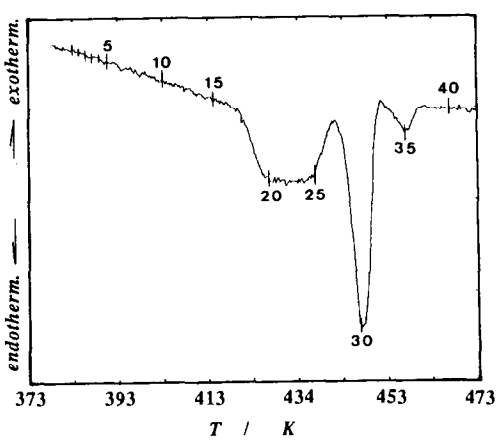

Fig. 6. DSC heating curve of PVDF/PMMA blend observed by simultaneous DSC/WAXD at 1 K min^{-1}.

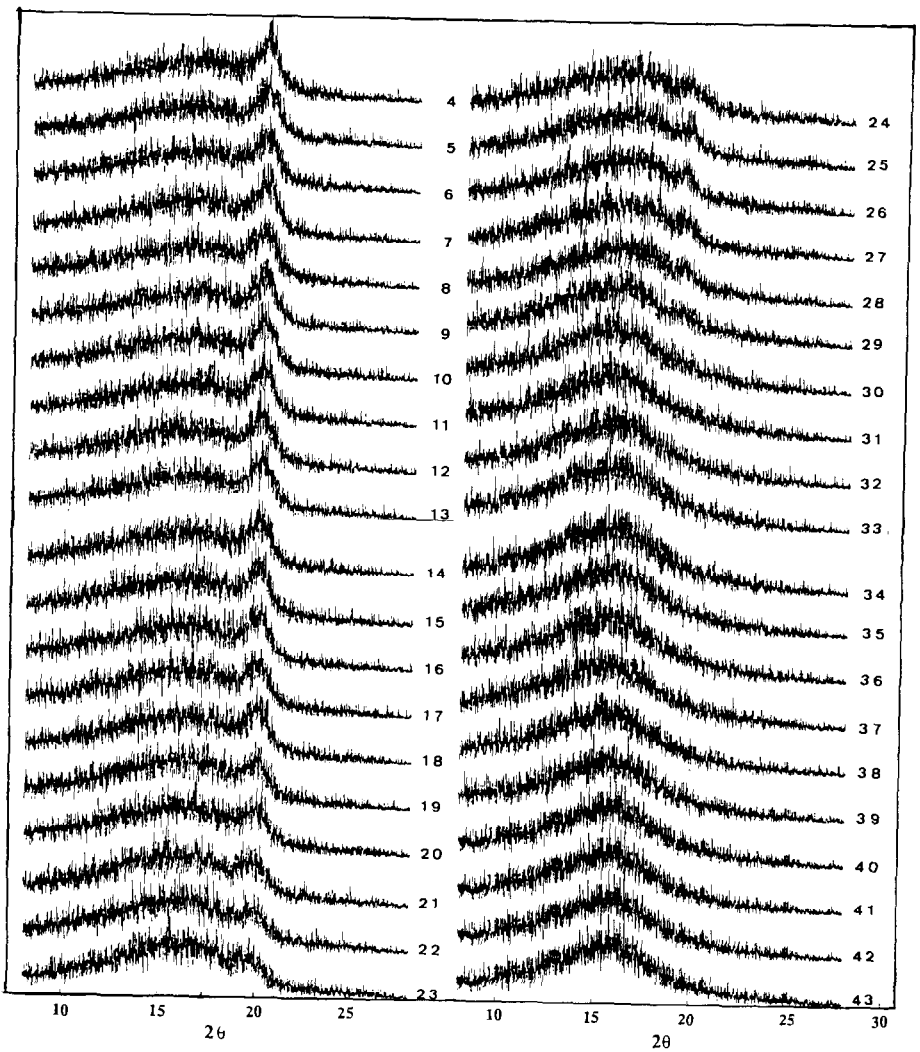

Fig. 7. WAXD profiles of PVDF/PMMA blend observed by simultaneous DSC/WAXD at 1 K min^{-1}. Numbers in the figure correspond to those on the DSC curve shown in Fig. 6.

at 20° consisted of at least two diffraction peaks whose peak positions were located above and below 20°. The WAXD profiles 26 and 27 indicated the presence of II(α)-modification. The diffraction peak at 19.4° disappeared completely at 446 K (WAXD profiles 29–31). The WAXD profiles 33 and 34 showed a small diffraction peak at 14° which was assigned to the (1 0 0) plane of the III(γ) modification. This small diffraction peak at 14° disappeared at 456 K (WAXD profile 35). These results suggest that the annealed PVDF/PMMA blend film originally contained I(β), II(α) and III(γ)-modifications,

and three endothermic peaks observed at 430, 446 and 456 K were due to the melting of I(β), II(α) and III(γ)-modifications, respectively.

Acknowledgements

The authors thank Professor Y. Yamamoto, Gunma University, for providing us with the sample of TG-iPP and Q-iPP.

References

[1] G. Ungar and J.L. Feijoo, Mol. Cryst. Liq. Cryst., 180B (1990) 281.
[2] G. Ungar, J.L. Feijoo, A. Keller, R. Yourd and V. Percec, Macromolecules, 23 (1990) 3411.
[3] A.J. Ryan, J. Thermal Anal., 40 (1993) 887.
[4] M. Kellens, W. Meeussen, R. Gehrke and H. Reynaers, Chem. Phys. Lipids, 58 (1991) 131.
[5] H. Chung and M. Caffrey, Biophys. Soc., 63 (1992) 438.
[6] H. Yoshida and M. Takahashi, Food Hydrocolloid, 7 (1993) 387.
[7] H. Yoshida, R. Kinoshita and Y. Teramoto, Thermochim. Acta, submitted.
[8] Y. Urabe, K. Takamizawa and T. Oyama, Rep. Prog. Polym. Phys. Jpn., 7 (1964) 109.
[9] Y. Urabe, K. Takamizawa and T. Oyama, Rep. Prog. Polym. Phys. Jpn., 8 (1965) 151.
[10] K. Tanaka, T. Seto and Y. Fujiwara, Reps. Prog. Polym. Phys. Jpn., 11 (1968) 285.
[11] Y. Fujiwara, Kolloid Z. Z. Polym., 226 (1968) 135.
[12] K. Kamide and K. Nakamura, Sen'i Gakkaishi, 25 (1987) 53.
[13] Y. Fujiwara, T. Goto and Y. Yamashita, Polymer, 28 (1987) 1253.
[14] Y. Yamamoto, M. Nakazato and Y. Saito, Netsu Sokuei, 16 (1989) 58.
[15] R. Hasegawa, Y. Takahashi, Y. Chatani and H. Tadokoro, Polymer J., 3 (1972) 600.
[16] A.J. Lovinger, J. Polym. Sci. Polym. Phys. Ed., 18 (1980) 793.
[17] C. Leonard, J.L. Halary and L. Monnerie, Polymer, 26 (1985) 507.
[18] H. Takimoto, Y. Sato, H. Yoshida, E. Ito and H. Hatakeyama, Polym. Preprints Jpn., 42 (1993) 1262.
[19] J. Lovinger, Polymer, 21 (1980) 1317.